J. Biomechanics Vol. 23, No. 7, pp. 687–703, 1990.
Printed in Great Britain

0021-9290/90 $3.00+.00
Pergamon Press plc

GONIOMETRIC MEASUREMENT OF HIP MOTION IN CYCLING WHILE STANDING

M. L. HULL, ANDREW BEARD and HEMANT VARMA
Department of Mechanical Engineering, University of California, Davis, CA 95616, U.S.A.

Abstract—The purpose of this study was to develop an instrument for quantifying the motion of the hip relative to the bicycle while cycling in the standing position. Because of the need to measure hip motion on the road as well as in the laboratory, a goniometer which locates the hip using spherical coordinates was designed. The goniometer is presented first, followed by the development of the equations that enable the distance from the joint center to the pedal spindle to be determined. The orientation of this line segment is specified by calculating two angles referenced to the frame. Also outlined are the procedures used to both calibrate the goniometer and perform an accuracy check. The results of this check indicate that the attachment point of the goniometer to the rider can be located to within 2.5 mm of the true position.

The goniometer was used to record the hip movement patterns of six subjects who cycled in the standing position on a treadmill. Representative results from one test subject who cycled at 6% grade and 25 km h^{-1} are presented. Results indicate that the bicycle is leaned from side to side with the frequency of leaning equal to the frequency of pedalling. Extreme lean angles are $\pm 6°$. The distance from the hip to the pedal varies approximately sinusoidally with frequency equal to pedalling rate and amplitude somewhat less than crank arm length. The absolute elevation of the hip, however, exhibits two cycles for each crank cycle. Asymmetry in the plot of elevation over a single crank cycle indicates that the pelvis rocks from side to side and that the elevation of the pelvis midpoint changes. Extreme values of the pelvis rocking angle are $\pm 12°$. Highest pelvis midpoint elevations, however, do not occur at the same crank angles as those angles at which the pelvis rocking is extreme. It appears that the vertical motion of the hips affects pedalling mechanics when cycling in the standing position.

NOMENCLATURE

$\bar{x}, \bar{y}, \bar{z}$	three orthogonal axes located at goniometer origin
x, y, z	three orthogonal axes located at intersection of the projection of the crank spindle and plane parallel to the plane of the frame passing through center of pedal platform
x_p, y_p, z_p	three orthogonal axes parallel to other coordinate systems but affixed to the center of the pedal spindle
R	radius of goniometer
α	angle between radius of goniometer and $\bar{x}$–$\bar{y}$ plane
β	angle between projection of radius on $\bar{x}$–$\bar{y}$ plane and $\bar{x}$–$\bar{z}$ plane
$\bar{x}_t, \bar{y}_t, \bar{z}_t$	location of goniometer attachment point in $\bar{x}, \bar{y}, \bar{z}$ coordinate system
x_s, y_s, z_s	location of $\bar{x}, \bar{y}, \bar{z}$ in x, y, z coordinate system
x_t, y_t, z_t	location of goniometer attachment point in x, y, z coordinate system
L_c	crank arm length
x_{pb}, y_{pb}, z_{pb}	location of x, y, z coordinate system in x_p, y_p, z_p coordinate system
x_{pt}, y_{pt}, z_{pt}	location of goniometer attachment point in x_p, y_p, z_p coordinate system
$\overline{TP}$, TP	line and distance respectively from goniometer attachment point to center of pedal spindle
AFORPED_t	angle formed between the z_p axis attached to the pedal spindle and the projection of $\overline{TP}$ on the x_p–z_p plane (from z_p axis counterclockwise)
AOUTPLN_t	angle formed between the plane of the frame and the projection of $\overline{TP}$ on the y_p–z_p plane (from plane of frame clockwise)
HIPD	distance from goniometer attachment point to the closest hip joint center
x_{2d}	two-dimensional fore/aft coordinate of goniometer attachment point
z_{2d}	two-dimensional elevation coordinate of goniometer attachment point
γ	estimate of bike lean angle (from vertical, counterclockwise)
$\bar{x}_h, \bar{y}_h, \bar{z}_h$	coordinates $\bar{x}_t$, $\bar{y}_t$, and $\bar{z}_t$ modified to locate hip joint center
θ	crank arm angle (from vertical, counterclockwise)
$\overline{HP}$, HP	line and distance respectively from hip joint center to center of pedal spindle
AOUTPLN_h	angle formed between the plane of the frame and the projection of $\overline{HP}$ on the y_p–z_p plane (from plane of the frame, clockwise)
C_0	offset constant used in computing bicycle lean angle
CSH	crank spindle height above the road surface with lean angle = 0
PO	pedal offset measured as the perpendicular distance from the center of the pedal to the plane of the bicycle frame
x_{ph}, y_{ph}, z_{ph}	coordinates of hip joint center in x_p, y_p, z_p coordinate system
x_h, y_h, z_h	coordinates of hip joint center in x, y, z coordinate system

Received in final form 28 *November* 1989.

INTRODUCTION

The desire for athletes to perform at their potential motivates not only athletes and coaches but also researchers who strive to gain scientific understanding. Scientific study benefited cyclists early, when the work of Sharp (1896) was published. Since that time,

an accumulation of published work has developed a better understanding of cycling. For some (e.g. Wong and Hull, 1983), the area of interest focused on bicycle mechanics. For others (e.g. Ericson *et al.*, 1986), biomechanical studies were the key to understanding the interaction of bicycle and rider. Either route shares seated cycling as the principle case of investigation. In many instances the knowledge gained has enabled a rational approach to bicycle equipment design, as the work of Okajima (1983) attests.

Extending the level of understanding of seated cycling that has been developed to the standing case requires a means of tracking hip position. Tracking the hip would enable the five-bar model (thigh, shank, foot, crank, seat tube) of a seated cyclist, presented by Redfield and Hull (1986), to be extended to the standing situation. For this situation the model would remain a five-bar linkage except that the degrees of freedom would increase. Because the hip would no longer be fixed but rather would be free to translate in the plane of leg flexion, the linkage would have four degrees of freedom. Information regarding hip position in conjunction with pedal load and pedal position data would enable a variety of biomechanical analyses such as computations of intersegmental loads.

Limited efforts have been focused on the subject of cycling while standing. Measurements of bike lean and lower back motion from cine films were made by Soden and Adeyefa (1979). The results indicate that the lower back displaces 13 cm vertically at twice the pedalling frequency. Maximum displacements occur when the crank arm is horizontal during the crank cycle. Focusing on hill climbing, Miller *et al.* (1988) relied on cine film to perform a more detailed kinematic analysis of cycling while standing. Using a treadmill, four position/cadence combinations were investigated to determine variations in kinematic variables between standing and seated positions. The kinematic variables studied included the range and mean of trunk rotation and hip, knee and ankle flexion angles and the displacement of the body's center of mass and rear hub acceleration.

Completed work related to cycling while standing could be related to hip motion, but the available work is not sufficient to specify the location of the hip vs crank position. Before biomechanical analysis of cycling while standing can begin, the geometric variables that must be specified include the crank and pedal angles as well as the length and orientation of the line connecting the hip to the pedal. Although video based methods such as that used by Miller *et al.* (1988) could be used to track hip location, these methods are not suitable for on-the-road testing, where the camera must be either inertial or referenced to the bicycle. The objectives of the project reported by this article were to both design and demonstrate the use of an electromechanical goniometer that could monitor hip motion either in the laboratory or on the road to study realistic cycling situations.

METHODS

Design description

In order to produce a goniometer that would measure representative displacements, the following design criteria were specified:

(1) The goniometer displacement data must be synchronized in time with crank angle and pedal angle data.

(2) The goniometer accuracy should exceed the accuracy to which anthropometric parameters can be specified.

(3) The goniometer must be easily set up on different bicycles.

(4) The goniometer must allow transition between different riding postures (i.e. seated or standing).

(5) The goniometer inertia and drag should not cause the goniometer attachment to shift due to soft tissue movement.

(6) The goniometer mass and placement should not increase the rotational inertia of the bicycle about the tire contact lines by more than 1 $kg\,m^2$.

To meet the design criteria, the goniometer incorporates four elements which determine hip location using spherical coordinates. Illustrated in Fig. 1, the four elements are titled attachment or tip, radius, origin and frame. The attachment consists of a thin copper sheet that is formed to the rider's side. This plate and an attached spherical bearing are fixed to the rider such that the center of the spherical bearing lies on a bony landmark which serves as a reference from which the hip can be located. The spherical bearing allows three angular degrees of freedom but no translation relative to the bony landmark. The radius of the goniometer curves from the attachment around the rider and extends behind the rider to link the attachment of the goniometer to the origin. The origin houses three potentiometers and associated bearings. Potentiometers measuring the two angles mount directly to axes of rotation. The distance from the attachment point to the origin is measured by transforming linear motion to rotational motion via a pinion that turns on a chain imbedded into and along the length of the radius. The pinion drives the shaft of a third potentiometer. At the origin, two linear bearings support the radius and allow it to pass through the intersection of the other two perpendicular rotational axes. The frame of the goniometer supports the origin in a convenient location behind and above the saddle by clamping to the seat post.

In considering the sources of error in making the hip measurement, the two that are attributable to the goniometer are inherent error and error due to soft tissue motion. One cause of soft tissue motion is force developed at the goniometer attachment when the rider moves. The goniometer offers several features which reduce this force. Firstly, the inertia of the radius is kept small by using a hollow shaft. Secondly, all three degrees of freedom are supported by low friction needle bearings as noted above. Finally, the

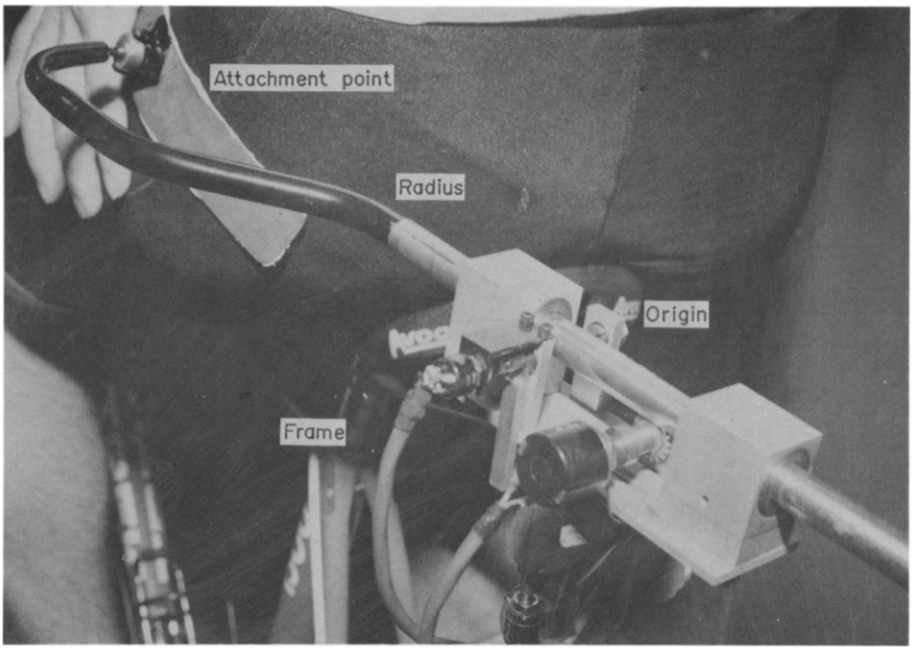

Fig. 1. Goniometer as attached to bicycle. Labeled components include: goniometer attachment point radius, origin and frame.

radius is counterbalanced so that when the rider is not moving, no force is transmitted by the attachment. The weight of the radius assembly including attachment hardware and counterbalance is 0.33 kg.

Equation development

Since the design locates the goniometer attachment using spherical coordinates, a mathematical procedure had to be developed to derive the hip-to-pedal-spindle distance and the orientation of this chord to the bicycle. To facilitate the mathematical derivation, three coordinate systems were established as shown in Fig. 2. The origin of the coordinate system denoted by $\bar{x}$, $\bar{y}$, $\bar{z}$ coincides with the goniometer origin. For this coordinate system α represents the angle between the radius of the goniometer and the $\bar{x}$–$\bar{y}$ plane. Angle β is measured from the $\bar{x}$–$\bar{z}$ plane to the projection of the radius onto the $\bar{x}$–$\bar{y}$ plane. The two planes and radius intersect at the origin. Another coordinate system, with axes parallel to those at the origin, is denoted by x, y, z. This coordinate system is located at the point where the projection of the crank spindle intersects the plane formed by the center of the pedal as it rotates with the crank arm. Attached at the center of the pedal spindle, the final coordinate system denoted by x_p, y_p, z_p translates with the pedal spindle but the axes remain parallel to those of the other two systems. The location of the coordinate system of the origin, relative to the coordinate system of the crank spindle, remains fixed during riding and is determined with the aid of levels and a plumb bob.

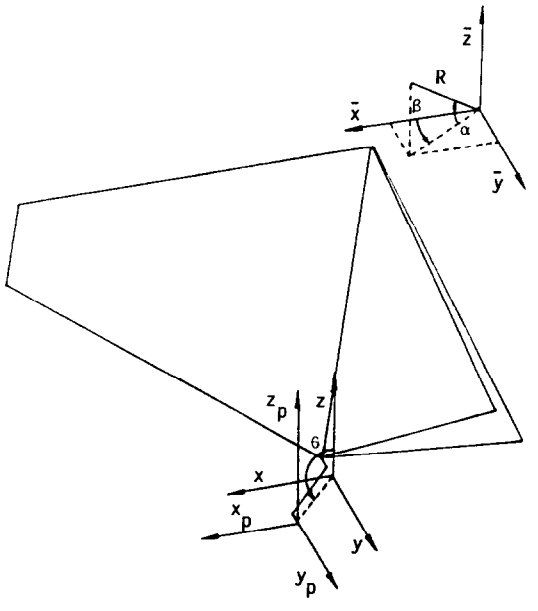

Fig. 2. Three coordinate systems used in equation development. $\bar{x}, \bar{y}, \bar{z}$ axes are used to convert measured polar coordinates into local Cartesian coordinates. x, y, z axes are used to locate either the attachment point or hip relative to the crank spindle and x_p, y_p, z_p locate either the attachment point or hip relative to the pedal spindle.

Transforming the measured polar coordinates to the desired hip-to-pedal spindle distance and line segment orientation requires that the attachment point to pedal spindle distance and orientation of this line segment be determined first. Making these determinations involves a multi-step procedure. The first of these steps converts the polar coordinates to Cartesian coordinates in the origin's coordinate system as follows:

$$\bar{x}_t = R\cos\alpha\cos\beta \tag{1}$$

$$\bar{y}_t = R\cos\alpha\sin\beta \tag{2}$$

$$\bar{z}_t = R\sin\alpha. \tag{3}$$

As a second step the goniometer attachment point is located relative to the crank spindle. To do this, the local coordinates of the attachment point found in equations (1)–(3) are used in addition to set-up coordinates. Designated as x_s, y_s, and z_s, the set-up coordinates locate the origin relative to the crank spindle and remain fixed for any one set-up. Using this notation, the coordinates of the goniometer attachment point in the crank spindle coordinate system are:

$$x_t = -x_s + R\cos\alpha\cos\beta \tag{4}$$

$$y_t = -y_s + R\cos\alpha\sin\beta \tag{5}$$

$$z_t = z_s + R\sin\alpha. \tag{6}$$

The next step requires that the crank spindle coordinate system be located with respect to the rotating pedal spindle. Since the transverse location of the crank spindle coordinate system origin coincides with the center of the pedal platform, the transverse coordinate is zero while the other two coordinates depend on crank arm angle θ. The coordinates x_{pb}, y_{pb}, z_{pb} of the crank spindle coordinate system origin are given by:

$$x_{pb} = -L_c\sin\theta \tag{7}$$

$$y_{pb} = 0 \tag{8}$$

$$z_{pb} = -L_c\cos\theta. \tag{9}$$

With the location of the bottom bracket specified, the position coordinates x_{pt}, x_{pt}, z_{pt} of the goniometer attachment point become:

$$x_{pt} = -L_c\sin\theta - x_s + R\cos\alpha\cos\beta \tag{10}$$

$$y_{pt} = -y_s + R\cos\alpha\sin\beta \tag{11}$$

$$z_{pt} = -L_c\cos\theta + z_s + R\sin\alpha. \tag{12}$$

Now the distance, TP, from the goniometer attachment point to the center of the pedal spindle can be determined from

$$TP = (x_{pt}^2 + y_{pt}^2 + z_{pt}^2)^{1/2}. \tag{13}$$

Having determined the length of the line segment that connects the goniometer attachment point to the pedal spindle, the final step is to find the orientation of this line segment. Finding this orientation requires quantifying two angles. The first represents a rotation

about the pedal spindle axis. Measured between the z_p axis and the projection of $\overline{TP}$ on the x_p–z_p plane, this angle is designated angle AFORPED$_t$. The second angle, AOUTPLN$_t$, determines the rotation between the plane of the frame and the projection of $\overline{TP}$ on the y_p–z_p plane. The two angles illustrated in Fig. 3 are determined from:

$$\text{AFORPED}_t = \tan^{-1}\left(\frac{x_{pt}}{z_{pt}}\right) \tag{14}$$

$$\text{AOUTPLN}_t = \tan^{-1}\left(\frac{y_{pt}}{z_{pt}}\right). \tag{15}$$

In order to determine the position of the hip in the pedal fixed coordinate system, the hip position relative to the goniometer attachment point must be found. Recognizing that this position must be determined from anatomical landmarks, two attachment points are possible. One is the anterior/superior illiac spine (ASIS) and the other is the superior aspect of the greater trochanter (SAGT) which lies along the hip axis of rotation during flexion/extension movements. The point selected was the SAGT because of complications in determining hip position relative to ASIS due to rotations of the pelvis.

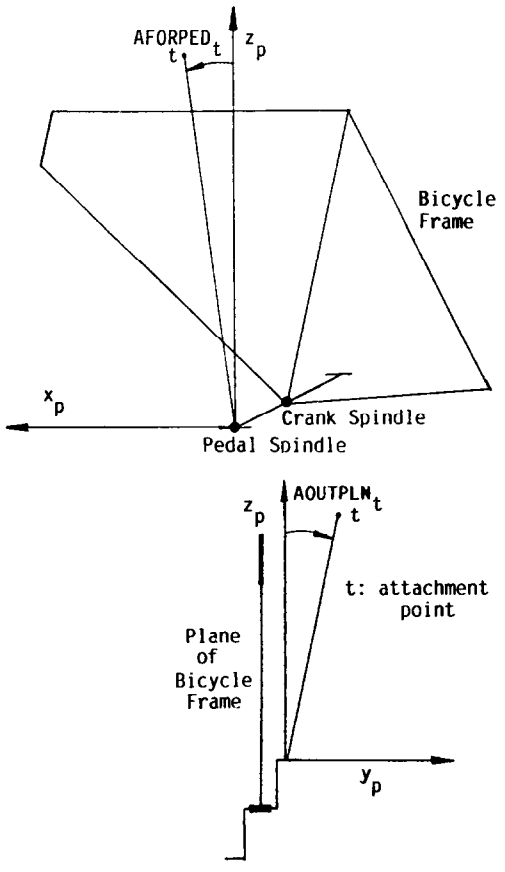

Fig. 3. Two angles that orient line segment connecting attachment point to pedal. AFORPED$_t$ is in plane of frame and AOUTPLN$_t$ is measured out of the plane of the frame.

With the attachment point specified, both the distance from the attachment point to the hip joint and the orientation of this line segment must be known. Denoted by HIPD, the distance may be obtained by either of two methods. One method is to assume that hip spacing is equal to pedal spacing, and then compute HIPD from the AOUTPLN$_t$ angle measured during seated cycling. In this method, y_{pt} in equation (15) is equal to HIPD. Because the pelvis width of adults may vary as much as 6 cm, the accuracy of this method is limited. A more accurate alternative method is to determine hip joint center from anatomical landmarks. The specifics of a procedure for doing this are detailed by Tylkowski *et al.* (1982).

With the attachment point to hip joint center distance specified, the coordinates that locate the attachment point can be modified to locate the joint center provided that the orientation of the line segment connecting the two points is known. To define this orientation, it is assumed that this segment both remains horizontal and does not rotate in the horizontal plane. Necessary to insure that the segment remains horizontal is the condition that leg movement be confined to a vertical plane. Also, the line will not rotate in the horizontal plane provided that the orientation of the vertical plane of leg movement remains fixed in space. To check these conditions, a preliminary study was undertaken where subject leg movement during standing cycling on a treadmill was viewed from the frontal plane using a video-based motion analysis system. Video results showed that the legs remain essentially vertical despite the leaning of the bicycle, and further that the orientation of the plane of movement does not change notably. Accordingly, the line segment connecting the attachment point to the hip remains horizontal even though rocking and/or twisting of the pelvis may occur (see Fig. 4). Thus, the two assumptions necessary for accurately estimating the center of the proximal hip joint are valid. The distal hip joint, however, is in an unknown position. If the location of this hip is needed, then symmetry may be assumed and the position determined by examining the known hip position 180° prior to the current position.

With the orientation specified, the modified position coordinates may be determined from one of two methods. One method is to modify the spherical coordinates while the second, and much simpler, method is to modify the Cartesian coordinates in the $\bar{x}$, $\bar{y}$, $\bar{z}$ coordinate system. The modified Cartesian coordinates $\bar{x}_h$, $\bar{y}_h$, $\bar{z}_h$ become

$$\bar{x}_h = \bar{x}_t \tag{16}$$

$$\bar{y}_h = \bar{y}_t - \text{HIPD}\cos\gamma \tag{17}$$

$$\bar{z}_h = \bar{z}_t + \text{HIPD}\sin\gamma \tag{18}$$

where γ is the lean angle of the bicycle to be defined shortly. With the coordinates that locate the joint center, the distance HP from joint center to pedal spindle and angle out of plane AOUTPLN$_h$ can be

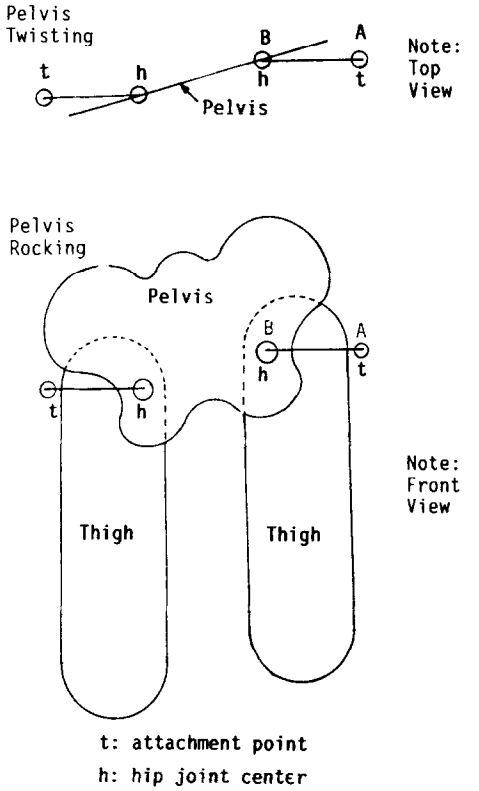

Fig. 4. Orientation of attachment point to proximal hip joint. As pelvis rotates about a line perpendicular to plane of paper and passing through (B), point (A) does not move.

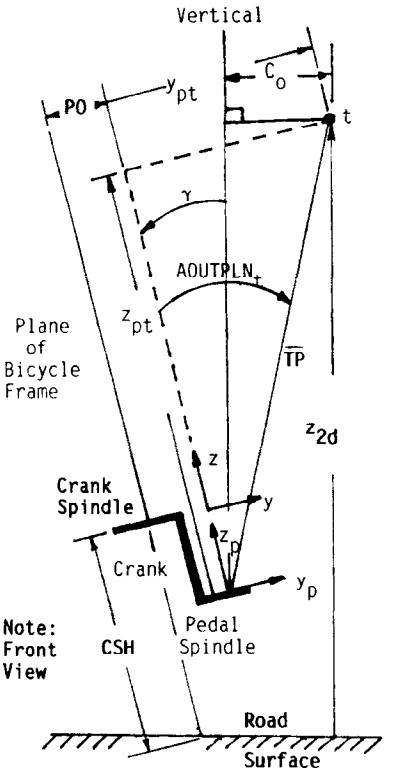

Fig. 5. Geometry viewed from the front as the bicycle leans to the rider's right. Bicycle lean angle γ is measured from vertical to the plane of the frame. The two-dimensional elevation coordinate z_{2d} is the perpendicular distance from the attachment point to the road surface.

determined by substituting the new coordinate values back into equations (10)–(12) and recomputing equations (13) and (15). The value of AFORPED will not change for the joint center values of $\bar{x}_h$, $\bar{y}_h$, and $\bar{z}_h$.

During cycling while standing, the bicycle is typically leaned from side to side. To estimate the lean angle γ of the bicycle, equation (15) is modified by including an offset constant such that γ has a zero value for seated cycling. The constant C_0 equals y_{pt} during seated cycling. If the first of the procedures described for finding HIPD is used, then C_0 also equals HIPD. Again, assuming that a line segment of length C_0 directed inwards from the attachment point remains horizontal, and also assuming that the point at the end of this line segment remains directly above the crank spindle coordinate system, according to Fig. 5, the bicycle lean angle is related to the constant C_0 by:

$$\tan\gamma = \frac{y_{pt} - C_0/\cos\gamma}{z_{pt}}. \tag{19}$$

For small lean angles (i.e. $<10°$), $\cos\gamma \to 1$ and $\sin\gamma \to \gamma$, reducing equation (19) to:

$$\gamma \approx \frac{y_{pt} - C_0}{z_{pt}}. \tag{20}$$

As noted earlier, assuming that the line segment of length C_0 remains horizontal is valid from video analysis. Also valid from video analysis is the assumption that the point at the end of this segment remains directly above the pedal in the frontal plane despite leaning of the bicycle.

For qualitative analysis, two-dimensional plots of the attachment position are useful. These plots give both the elevation and the fore/aft position of the attachment point. Elevation is the perpendicular distance to the road surface while fore/aft position is along the x axis of the crank spindle coordinate system. With the bicycle lean angle estimated, the two-dimensional position coordinates can be determined. Since the fore/aft position is unaffected by bicycle lean, the only additional computation is for the elevation coordinate. Referring to Fig. 5, the fore/aft and elevation coordinates, x_{2d} and z_{2d} respectively, are found from:

$$x_{2d} = x_t \tag{21}$$

$$z_{2d} = z_{pt}/\cos\gamma + C_0\tan\gamma - z_{pb}\cos\gamma + \mathrm{CSH}\cos\gamma + \mathrm{PO}\sin\gamma. \tag{22}$$

For small γ, equation (22) reduces to:

$$z_{2d} = z_{pt} - z_{pb} + \mathrm{CSH} + C_0\gamma + \mathrm{PO}\gamma. \tag{23}$$

In the equations above, CSH is the crank spindle height above the road surface with zero lean angle and PO is the pedal offset (perpendicular distance from the

pedal center to the plane of the bicycle frame). Typical values for CSH and PO are 28 cm and 13 cm respectively.

CALIBRATION AND ACCURACY CHECK

Before the hip to pedal distance can be determined, the values of R, α and β that locate the attachment point must be determined from the output voltages. This calibration process took place in two steps. The first step established a calibration coefficient for the potentiometers that measure rotation motion. To determine the slope of the line that relates voltage to degrees, known rotation inputs were applied and corresponding outputs measured. The second step relied upon a vertical mill to calibrate the linear motion of the radius. The attachment point was clamped to the mill so that angles α and β were zero and the radius was aligned with the lateral feed direction. Displacements were then read directly from the mill and related to the potentiometer voltages to establish a calibration coefficient. In addition to enabling calibration, the set-up verified that the goniometer axes were perpendicular. This was assured because the values of α and β remained at zero when the radius was taken through its full range of motion.

To assess the inherent error in the goniometer, an accuracy check was conducted again using the vertical mill. The eight corners of an imaginary rectangular box served as the data points. Located in a region where the hip will be located when cycling while standing, the box had dimensions characteristic of real hip motions (see Fig. 6). Angles α and β were set to zero at one point and the radius was determined with vernier calipers. The mill was then moved to the other points and data were recorded. To quantify the accuracy, the calibrated goniometer data were compared to the mill readings. The results from both the calibration and the accuracy check are presented in Table 1.

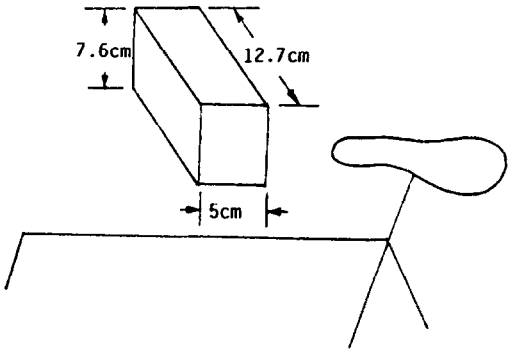

Fig. 6. Eight points used in accuracy check. Dimensions and orientation of box cover region where instrument will be used.

Because it is not feasible to rigidly attach the goniometer to the rider's thigh, a means of quantifying errors resulting from soft tissue motion was necessary. Soft tissue motion errors are traced to two sources. One source is the combined effects of radius inertia and bearing friction which cause a shear force to be developed at the goniometer attachment/skin interface. Of these effects, the radius inertia dominates. To determine the shear force due to inertia, the maximum absolute acceleration of the attachment point was estimated from two-dimensional position plots such as those illustrated in Fig. 10. This estimation was then combined with the radius mass to determine the shear force. For a radius mass of 0.33 kg and an acceleration of 6 m s^{-2}, the corresponding force is 2N. This force was then applied to the goniometer attachment point using a spring scale and the resulting movement of the attachment point was recorded to be less than 1.5 mm.

A second source of soft tissue motion error is traced to the movement of the skin over the greater trochanter as the leg is flexed and extended. To quantify this

Table 1. Results of calibration and accuracy check

Calibration:

Linear resolution = 0.2 mm
Rotation resolution = 0.15°
Noise level = 1 part in 2048

Accuracy check:

	Geometric calculation			As measured by goniometer		
Point	R(mm)	α(deg)	β(deg)	R(mm)	α(deg)	β(deg)
1	464.5	0	0	464.5	0	0
2	515.3	0	0	514.4	0	0
3	530.8	0	13.84	528.4	0	13.83
4	481.6	0	15.28	479.3	0	15.28
5	487.6	8.99	15.28	485.5	8.89	15.09
6	470.8	9.32	0	470.1	9.22	0
7	521.0	8.41	0	519.6	8.57	0
8	536.3	8.17	13.89	534.0	8.27	13.67

Max error in radius = 2.4 mm; max error in angles = 0.19°.

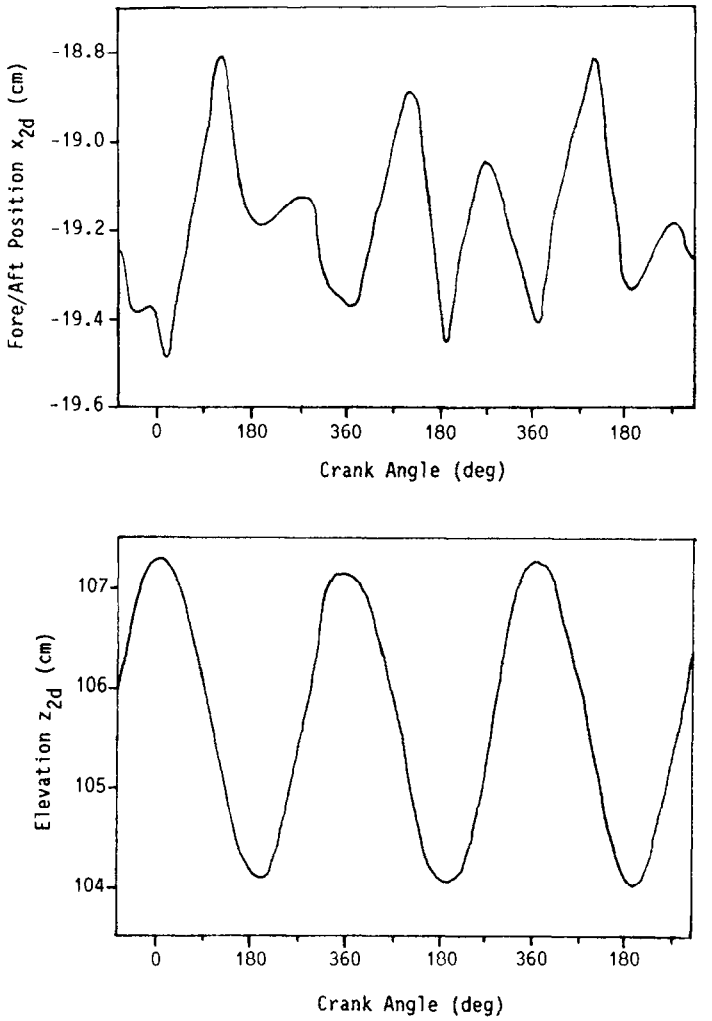

Fig. 7. Two-dimensional position coordinates when cycling at lower power in the seated position. The x_{2d} coordinate is fore/aft position while the z_{2d} coordinate is elevation. Since the pelvis does not move in this position, variations in these coordinates are due primarily to soft tissue movement. The variation in the z_{2d} coordinate is large enough to warrant correcting for this error.

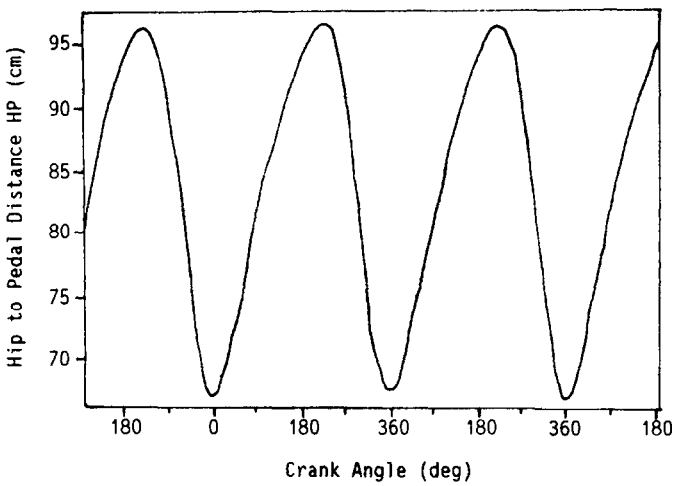

Fig. 8. Distance HP from the hip joint center to the origin of the pedal spindle fixed coordinate system. The pattern is approximately sinusoidal due to circular pedal path and small movements of the hip joint center. The range of distance is 30 cm, which is somewhat less than twice the length of the crank arm.

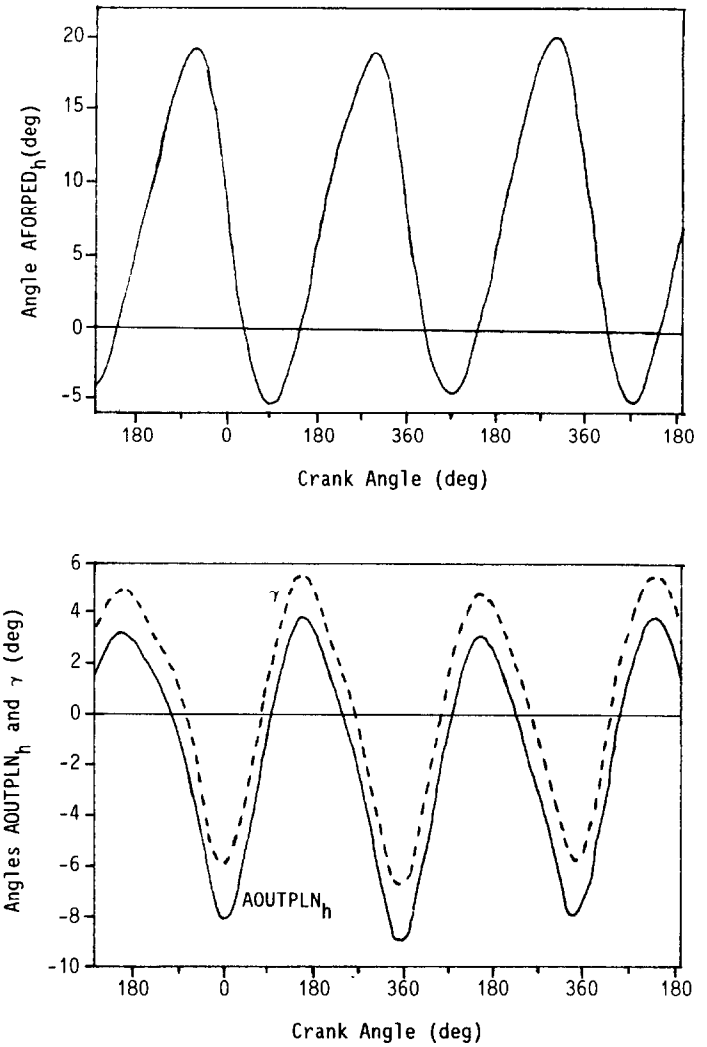

Fig. 9. Angles $AFORPED_h$ and $AOUTPLN_h$ defining the orientation of the line segment connecting the hip joint center to the origin of the pedal spindle coordinate system. The bicycle lean angle γ is also shown. A positive $AFORPED_h$ angle indicates that the hip is forward of the pedal spindle over the majority of the crank cycle. When the crank arm is 90° past top dead center, however, the angle is negative, indicating that the hip joint center is rearward of the pedal spindle. The bicycle lean angle indicates the lean of the bicycle from the vertical plane. A positive lean angle is to the rider's right. Lean angle sign corresponds to bicycle leaning to the side opposite of the leg in the power phase of the crank cycle. The angle $AOUTPLN_h$ is similar in pattern to the bicycle lean angle. The average value of $AOUTPLN_h$ is negative because the distance HIPD is greater than C_0, thus locating the hip center inboard of the center of the pedal.

error, the rider pedaled the bicycle slowly ($\sim$60 rpm) under low load ($<$100 W) in the seated position with the torso upright. This position approximates that of standing. During seated cycling at low power and slow pedaling rate, the pelvis is virtually stationary with respect to the bicycle (Komor *et al.*, 1985) so that any goniometer output is due to soft tissue motion. Although variations in the x_{pf} position coordinates were less than 1 cm, the z_{pf} coordinate varied by about 3 cm peak to peak. Because this variation in the z_{pf} coordinate represents a potentially large error, the z_{pf} coordinate data computed according to equation (12) were corrected using the data recorded during cycling in the seated position. With this correction, the absolute errors in all three position coordinates x_{pf}, y_{pf}, z_{pf} are estimated at $\pm$1 cm.

Having implemented the geometric relations given by the preceding equations into FORTRAN code, a means of verifying the program output was required. With the goniometer mounted to the bicycle and the various coordinate systems aligned, the goniometer attachment was fixed in space and located relative to the bottom bracket coordinate system. Running the program produced results for comparison. Because these results differed by no more than 2.5 mm, the program was working correctly.

During the gathering of data from experiments where the goniometer was used to monitor hip mo-

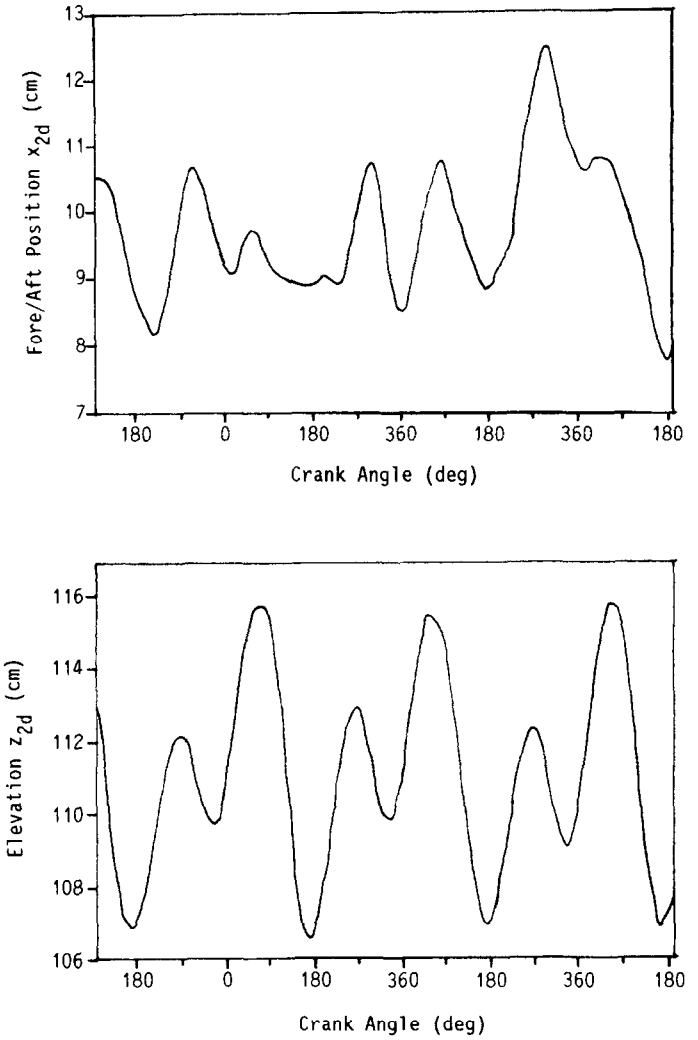

Fig. 10. Two-dimensional position coordinates when cycling in the standing position. The range of the x_{2d} coordinate (fore/aft position) is small, indicating that the hip does not move significantly relative to the bicycle in this direction. The z_{2d} coordinate exhibits two cycle behavior over a crank cycle. The disparity in maximum values occurs because of rocking of the pelvis about an anterior/posterior axis.

tion, both the crank angle θ and the pedal angle (not defined herein) were also measured. These angles were measured using potentiometers according to the procedures outlined in Hull and Davis (1981). To synchronize both goniometer and crank angle data and provide data in a form amenable to computer analysis, all potentiometer signals were sampled sequentially at 100 Hz/channel and digitized via a 12-bit analog-to-digital converter. The data acquisition process was controlled with an IBM PC/AT compatible computer.

Data were recorded during two separate experiments from six subjects all of whom were experienced cyclists. Table 2 lists the test subject data. One experiment involved seated cycling and the other standing cycling. Because the purpose of the seated cycling test was to obtain data which would indicate soft tissue movement, this test was conducted with the subject's bicycle mounted onto a windtrainer. The objective of the standing cycling test, on the other hand, was to record data representative of actual cycling in the standing position. Accordingly, this test was carried out on a treadmill at 6% grade and 25 km h^{-1}. During the standing cycling test, a cadence of approximately 72 rpm was maintained while riding a bicycle of racing quality. Also, the hands were grasping the brake hoods and the shoes were locked to the pedals.

Table 2. Test subject data

	MH	SW	MC	DH	CS1	CS2
Age (yr)	42	24	35	28	20	30
Weight (kg)	75.0	56.8	68.2	72.7	70.9	72.7
Height (m)	1.75	1.68	1.75	1.73	1.76	1.78

RESULTS

To illustrate both the type of data produced by the goniometer and how to interpret these data, sample results of a single test subject are shown in Figs 7–11. Figure 7 shows the results for seated cycling at low power while Figs 8–11 show the results for standing cycling.

Illustrated in Fig. 7 are the variations in the two-dimensional position coordinates of the goniometer attachment as a function of crank angle. Note that the angle of 0° corresponds to the top dead center position of the crank arm and that the reference goniometer attachment position is with the leg fully extended (i.e. crank arm angle = 180°). The plots in Fig. 7 indicate that the variation in the x_{2d} coordinate is small (< 1 cm) and that the pattern of movement is not consistent from cycle to cycle. Contrasted to this movement is that of the z_{2d} coordinate, which exhibits approximately sinusoidal variation, reaching an elevation about 3 cm above the reference position at the top dead center position of the crank. The relatively large variation in the z_{2d} coordinate indicates the desirability of correcting the position data. The high repeatability of the pattern of variation establishes the feasibility of making the correction reliably.

The next results to be presented are those that describe both the length of the line connecting the hip joint center to the pedal spindle coordinate origin and the orientation of this line relative to this origin.

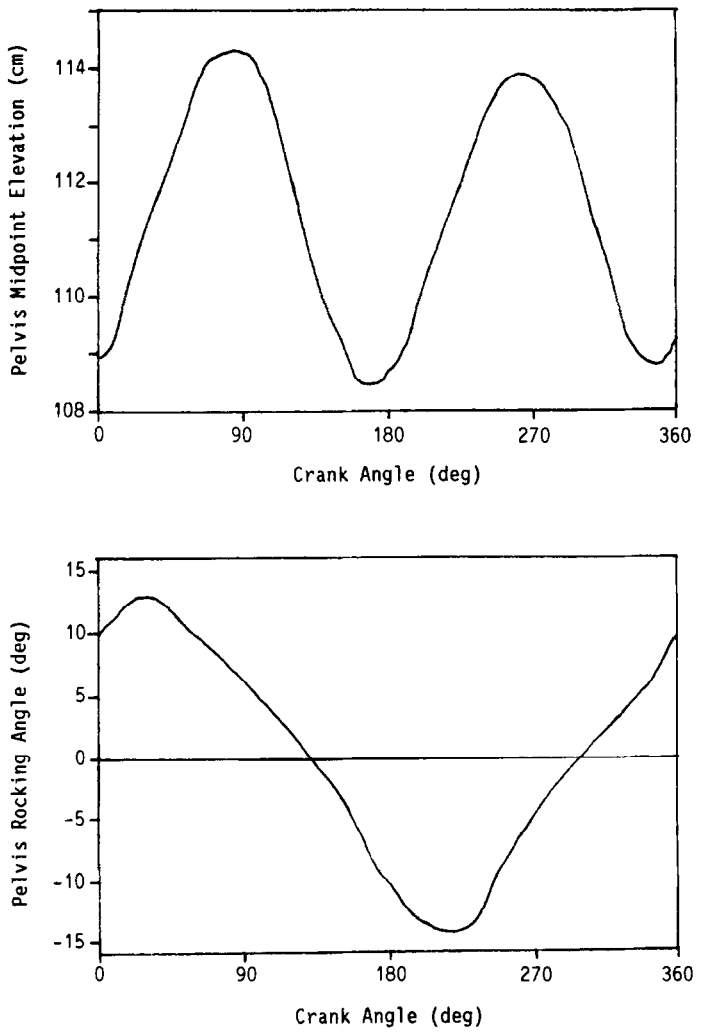

Fig. 11. Elevation of pelvis midpoint and pelvis rocking angle computed assuming left/right symmetry and using the z_{2d} data in Fig. 10. Changes in the pelvis midpoint elevation indicate loss and gain of potential energy of the torso. The two cycle behavior with highest elevations occurring midway through the power strokes of the cranks suggests that potential energy changes are important to cycling mechanics in the standing position. To gain a complete picture of pelvis movement, rotation in rocking must be considered in conjunction with vertical translation. Positive rocking angles correspond to the left hip higher than the right. Consistent phase difference between rocking angle extremes and highest midpoint elevations indicates natural coordination between these two modes of motion.

Presented in Figs 8 and 9 are the line length HP and angles respectively. The value of C_0 was determined from seated cycling to be 4.9 cm. The value of HIPD used in equations (16)–(18) was determined using the procedures outlined in Tylkowski *et al.* (1982) and was found to be 7.5 cm for the test subject. Also, the $\bar{z}_t$ coordinate data were corrected for soft tissue movement using the variation in z_{2d} from Fig. 7.

In examining the line length HP as a function of crank angle in Fig. 8, an approximately sinusoidal variation in length is observed with the minimum and maximum values occurring near the top and bottom dead center positions respectively of the crank. Because the top dead center position of the crank brings the pedal spindle closest to the hip, while the bottom dead center position removes the pedal spindle farthest, this phasing of the maximum and minimum lengths is expected. It may be noticed that the difference between maximum and minimum lengths is 30 cm which is approximately twice the length of the crank arm (17 cm).

Illustrated in Fig. 9 are the angles AFORPED_h, AOUTPLN_h, and γ as a function of crank angle. Examining first the plot of AFORPED_h, it is seen that this angle varies nearly sinusoidally with minimum and maximum values coinciding with the crank being midway through the power phase (0–180°) and midway through the recovery phase (180–360°) respectively. Nearly sinusoidal variation indicates that the x-position of the hip does not move significantly relative to the bicycle. The phasing apparent in Fig. 9 follows directly from the circular path of the pedal spindle. At 90°, the angle realizes a negative extreme indicating that the hip is rearward of the pedal spindle when the spindle is in its most forward position. At 270°, on the other hand, the angle reaches the positive extreme indicating that the hip is forward of the pedal spindle when the spindle is in its most rearward position.

Also illustrated in Fig. 9 is the angle AOUTPLN_h and the bicycle lean angle γ. It is noticed that the two plots resemble one another almost identically except that the average values are different. The average value of the bicycle lean angle is zero, which is expected providing that the rider both does not shift the distance C_0 during the transition from the seated to standing position, and leans the bicycle similarly from side to side. Because the HIPD value of 7.5 cm exceeds the C_0 value of 4.9 cm, the hip center is located inboard of the pedal center, thus giving rise to the negative average of HIPD.

Contrasted to the angle AFORPED_h which exhibits a regular pattern in both phase and amplitude, the bicycle lean angle pattern in Fig. 9 is irregular in amplitude but regular in phase. The irregularity in amplitude presumably stems from inconsistency in riding mechanics from crank cycle to cycle. Noting that positive lean angles correspond to the bicycle leaning to the rider's right, the bicycle is leaned to the right during the majority of the power stroke and to the left during the majority of the recovery stroke. Recognizing that the recovery stroke of the left crank corresponds to the power stroke of the right crank, the bicycle is leaned to the right when the left leg is producing maximum power and vice versa for the right leg. With the pedal being offset from the plane of the bicycle, the result of the leaning is to close the vertical distance between the hip and the pedal. Because the leg develops force on the pedal, closing this distance represents work done. This work is done by the arms which apparently assist the legs in developing peak power during cycling while standing.

The next results to be presented are those for the two-dimensional attachment point position coordinates during cycling while standing. These coordinates are illustrated in Fig. 10 as a function of crank angle over the same crank angle region as that in Figs 8 and 9. Inspecting first the plot for x_{2d} it is observed that the movement of the attachment point relative to the crank spindle along the x direction is small; the x_{2d} coordinate varies by only 4 cm. This result is expected from the earlier observation surrounding the close approximation of the AFORPED_h angle to a sinusoid. While the variation is small, the average value is between 9 and 10 cm, indicating that the attachment point is forward of the crank spindle for this subject. The cycle to cycle pattern is not consistent. Given the small variation in this coordinate, inconsistency in the pattern would result from slight differences in cycling mechanics from cycle to cycle.

Also illustrated in Fig. 10 is the z_{2d} coordinate indicating the elevation of the attachment point above the road surface. Contrasted to the x_{2d} coordinate, the z_{2d} coordinate exhibits a two-cycle pattern which is consistent from cycle to cycle. In this pattern the first peak occurs at about 45° with the second peak occurring 180° later in the cycle. Also the amplitude of the first peak is greater than the second. The cycle-to-cycle variation in the elevation is about 9 cm which suggests that the torso gains and loses potential energy.

Because the z_{2d} coordinate indicates the elevation of the attachment point and hence the hip above the road surface, both pelvis rocking angle and the elevation of the pelvis midpoint may be estimated by assuming that the elevation of the right hip is the same as the left only 180° out of phase. The difference between right and left hip elevations may be used to determine the rocking angle while the elevation of the pelvis midpoint is given by the average of the two hip elevations. Using the data points over the first full crank cycle in the z_{2d} plot of Fig. 10, plots of both the pelvis rocking angle and the average elevation of the pelvis midpoint were developed and are illustrated in Fig. 11.

With the elevation of the pelvis determined, it becomes possible to assess at least qualitatively the change in potential energy of the torso. From the plot of average pelvis elevation in Fig. 11, it is clear that this elevation exhibits two-cycle behavior over each crank cycle. Potential energy is greatest at crank angles of 80° and 260° and least at crank angles of 170° and 350°. Maximum powers of the left and right

cranks typically occur near 100° and 280° respectively. Accordingly, the torso reaches greatest potential energy just prior to maximum power, and loses potential energy as maximum power is developed. Recall also that the bicycle lean angle (see Fig. 9) is phased such that the bicycle is leaned away from the leg developing maximum power. Consequently, it appears that both work done by the arms and upper body potential energy changes are important factors in the mechanics of cycling in the standing position.

Complicating the description of pelvis movement is rotation of the pelvis in rocking, which occurs simultaneously with vertical translation. However, the plot in Fig. 11 indicates that the rocking angle goes through a single cycle for each crank cycle as opposed to two cycles. Noting that a positive rocking angle corresponds to the left hip being higher than the right, the left hip is maximally higher than the right when the left leg is 30° into its power stroke whereas the right hip is maximally higher than the left with the right leg 30° into its power stroke (i.e. angle of left crank 210°). Although extreme rocking angles occur earlier in the crank cycle than the highest pelvis midpoint elevations, the consistent phase between extreme angles and highest elevations suggests natural coordination between these two modes of motion.

Although the results presented in this paper are those of one subject, (MH), the goniometer was used to record the motion of five additional subjects. With the exception of the x_{2d} variables for both seated and standing cycling, the patterns of variation in all other variables were similar to those evident in the figures. Maximum and minimum values of the variables and the corresponding crank angles averaged over three crank cycles are listed in Table 3. As might be expected, differences in riding styles of subjects lead to some of the results being subject dependent. In particular one subject-dependent result was the position of the hip relative to the crank spindle. Some subjects, such as the one shown herein, stood in a more upright position with the result that the hip was generally well forward of crank spindle, whereas other subjects stood in a somewhat crouched position so that the hip was nearly over the crank spindle. As a consequence, the average values of both the $AFORPED_h$ angle and x_{2d} coordinate decreased from the average values in Figs 9 and 10 respectively.

Another subject-dependent result was the phase of the bicycle lean angle. Similar to the subject herein, four of the other five subjects developed extreme values approximately midway through the second half of the power stroke (see Table 3). One subject (SW), however, developed extreme values closer to the top and bottom dead center position of the cranks. Accordingly, rather than the bicycle being leaned to the right over the majority of the power stroke of the left crank as evident in Fig. 9, the bicycle was leaned to the left during the first half of the power stroke (0–90°) and to the right during the second half (90–180°).

DISCUSSION

In considering the errors in the measurements provided by the goniometer, it is necessary to distinguish between the errors in measuring the goniometer attachment point and the errors in determining the hip position. The sole error in measuring the goniometer attachment point is the inherent error which is quantified in Table 1. Beyond the inherent error, additional errors are encountered in determining the hip position. These errors include the uncertainty in locating the goniometer attachment along the hip axis of rotation, the shifting of the attachment point due to soft tissue movement, and the uncertainty in the distance HIPD from the attachment point to the hip joint center. Of these, the dominant errors are the shifting of the attachment point due to soft tissue movement and the uncertainty in the distance HIPD. The shifting of the attachment point may be reckoned with using the correction procedure outlined herein. To reduce the uncertainty in distance HIPD, this distance may be measured directly from a radiograph rather than estimated using the procedures of Tylkowski *et al.* (1982).

Another error source in locating the hip surrounds the assumptions regarding the relation between the goniometer attachment point and hip joint center. Recall that it was assumed that the line connecting the two both remains horizontal and does not rotate in the horizontal plane. These assumptions were confirmed through video review over the complete crank cycle. Consequently, results computed according to the equations presented herein are valid even though rocking of the pelvis occurs. In the event that the assumptions surrounding the orientation of the line segment connecting the attachment point to the joint center are not satisfied, errors will be introduced in determining the hip joint center. Since the goniometer design places the attachment point close to the skin, the attachment point to center distance is as small as possible. Consequently, the above errors will be minimized.

In view of the need to correct the position data due to soft tissue movement when the goniometer attachment point is located at the superior aspect of the greater trochanter (SAGT) which is along the axis of femur rotation in flexion/extension movements, the question naturally arises as to whether relocating the attachment point to the anterior/superior iliac spine (ASIS) would be preferable. In evaluating the choice of attachment point from the standpoint of minimizing errors, note that soft tissue movement is not the only concern; changes in orientation of the line segment connecting the attachment point to the hip joint are also a concern. If the point coincides with the SAGT, then the femur rotations (axial and abduction/adduction) must be considered. As was evident from the preliminary study where leg motion was studied via video, these femur rotations were minimal.

Table 3. Maximum and minimum values of variables and corresponding crank angles averaged over three crank cycles for the six subjects

		MH	SW	MC	DH	CS1	CS2
Seated							
x_{2d}	Max/min (cm)	−18.8/−19.5	−19.8/−21.1	−22.0/−22.6	−22.8/−23.3	−21.2/−22.1	−23.0/−23.8
z_{2d}	Max/min (cm)	107.2/104.2	105.5/103.2	107.4/104.8	105.5/102.9	112.0/109.6	109.6/105.0
	Crank angles*	0°/180°	10°/195°	10°/180°	0°/180°	0°/180°	0°/180°
Standing							
AFORPED	Max/min	+19°/−5°	+14°/−1°	+16°/−6°	+18°/−7°	+17°/−5°	+14°/−8°
	Crank angles*	290°/90°	310°/100°	270°/75°	280°/80°	290°/90°	280°/75°
$AOUTPLN_t$	Max/min	+8°/−2°	+8°/−6°	+8°/−2°	+6°/0°	+6°/−0.5°	+9°/−1°
	Crank angles*	135°/345°	180°/0°	135°/330°	130°/330°	165°/340°	145°/335°
$AOUTPLN_h$	Max/min	+3°/−8°	+4°/−11°	+4°/−8°	+1°/−5°	+2°/−6°	+3°/−8°
γ	Max/min	+5°/−6°	+6°/−6°	+6°/−6°	+2.5°/−3°	+3.5°/−4°	+5°/−5°
HP	Max/min (cm)	97/67	94/64	100/72	100/70	103/73	96/68
	Crank angles*	210°/0°	225°/10°	200°/350°	205°/350°	210°/355°	215°/355°
x_{2d}	Max/min (cm)	12.5/8	5.5/1	9/4	10.5/5	10.5/6.5	6/1.5
z_{2d}	Max/min (cm)	116/107	111/104	119/109	117/108	122/113	116/105.5
	1st peak	115 cm/50°	111 cm/80°	119 cm/45°	117 cm/45°	122 cm/45°	116 cm/50°
	1st valley	107 cm/165°	104 cm/180°	109 cm/160°	108 cm/106°	113 cm/160°	106 cm/170°
	2nd peak	112 cm/260°	108 cm/270°	114 cm/260°	114 cm/260°	117 cm/255°	112 cm/270°
	2nd valley	110 cm/330°	104 cm/360°	112.5 cm/315°	111 cm/320°	115 cm/320°	110 cm/320°

* First angle corresponds to maximum variable value.

If the attachment point coincides with the ASIS, then rotations of the pelvis merit attention. The three rotations of the pelvis are tilt (rotation about a line connecting the two ASISs), rocking (rotation about a line perpendicular to the tilt axis and directed anteriorly/posteriorly with the person in the anatomical position) and twist (rotation about a line mutually perpendicular to the other two rotation axes). Note that the terminology used herein for these rotations is different from that used by Tylkowski *et al.* (1982) because the definition of the axis system is different. Under the symmetry assumption, it is possible to estimate both the rocking and twist angles from the data presented herein. Pelvis rocking may be estimated from the difference in elevations 180° apart in the crank cycle, whereas pelvis twist may be estimated from the difference in fore/aft positions. Both angles are estimated to range approximately between $\pm 10°$.

With the rocking and twist angles estimated, it is possible to compute errors introduced by pelvic rotations. From the ASIS to the hip joint center, the largest distance is along the axis directed anteriorly/posteriorly (Tylkowski *et al.*, 1982). Assuming that spacing between ASISs is 27 cm and that 21% of this distance locates the hip center posteriorly of the ASIS, the error introduced in the $\bar{x}_h$ coordinate for a 10° twisting angle would be 1 cm. Inasmuch as the distance locating the hip joint center inferiorly to the ASIS is about half that of the posterior distance and the rocking angle is the same as the twisting angle, the error in the $\bar{z}_h$ coordinate is about 1/2 cm.

While the errors above are probably within acceptable limits, keep in mind that an additional error would be introduced by pelvis tilt. Unfortunately, it is not possible to quantify the tilt angle from the data presented herein so that levels of error cannot be computed. It is probable, however, that an angle of tilt is assumed in the standing position since the body is in a forward leaning position and further, that this angle varies somewhat. Tilt angle would manifest itself as a further error in the $\bar{x}_h$ coordinate. Inasmuch as the total variation in this coordinate is about 5 cm, the corresponding relative error would become large.

In the final analysis, the choice of attachment point represents a trade-off. Choosing the SAGT minimizes orientation errors at the expense of larger soft tissue motion errors, while choosing ASIS does the reverse. Because soft tissue motion errors can be readily corrected, attaching the goniometer to the SAGT allows both the x_{ph} and z_{ph} coordinates to be determined with comparable absolute error of 1 cm. Attaching the goniometer to the ASIS, however, would lead to similar absolute error in z_{ph} but probably larger absolute error in x_{ph} due to pelvic rotations.

The question of exactly what level of error is tolerable in these position measurements has not yet been answered, to the authors' knowledge. In order to answer this question, it appears necessary to perform a sensitivity analysis which studies the effect of position coordinate uncertainty on lower limb kinematics and ultimately intersegmental loads.

Looking to the goal of determining intersegmental loads, the position coordinates yielded by the procedure described herein may not be sufficient kinematic information to compute these loads. This is because these coordinates are measured with respect to the bicycle which is not an inertial reference. Accelerations occur not only along the y and z axes due to bicycle lean, but also along the x axis due to fluctuations in crank torque. While accelerations along the y and z axes may be computed knowing lean angle, pedalling rate, and bicycle geometry, the acceleration along the x axis would require a separate measurement. Inasmuch as determining intersegmental loads requires pedal load measurements as well as hip position measurements, acceleration along the x axis could be determined by computing crank torque from the measured pedal loads. Consequently, with the accelerations of the bicycle known and the relative accelerations of the attachment point available by differentiating position coordinates, the absolute accelerations of the attachment point may be found.

Although there are no data available of hip motion for comparison to the presented results, the motion of both the bicycle and the lower back as studied by Soden and Adeyefa (1979) can be compared. To describe lower back motion from the results presented herein, refer to Fig. 11, which illustrates the average elevation of the pelvis. Since the average indicates the elevation of the pelvis midpoint, obtaining the elevation of the lower back necessitates adding an appropriate constant. This constant need not be included, however, if only relative motion over the crank cycle is of interest. It is evident from the figure that the average reaches a maximum elevation with the cranks near 80° and 260°, and the change in elevation is approximately 5 cm. This change in elevation is representative of all the other subjects. The phase of extreme values is representative for four of the five other subjects; one subject (SW) developed extreme values somewhat later in the crank cycle. Reporting maximum elevations at about 70° and 250°, the results of Soden and Adeyefa (1979) regarding phasing of extreme values are consonant with those here. However, Soden and Adeyefa also reported a change in elevation of approximately 13 cm, which is notably larger than the change for all of the subjects here. With regard to bicycle lean angle, Soden and Adeyefa found the angle to range between $\pm 10°$ and the extreme values occurred with the cranks at top and bottom dead center. One of the subjects used here exhibited this phase but none of the subjects developed lean angles approaching 10° in amplitude.

The differences between the results of Soden and Adeyefa (1979) and these herein are likely to be due to two factors. One factor is the cycling situation. Although the cadence and gear ratio were comparable between the two studies, Soden and Adeyefa had subjects cycle a steeper grade (10%) with the hands on

the handlebar drops rather than the brake lever hoods. The considerably higher work level in conjunction with the more crouched riding position could account for the greater lean angle and greater lower back elevation change. A second factor surrounds the accuracy of the procedures used to make these measurements. Measurements were made from cine film. Soden and Adeyefa (1979) acknowledged that the accuracy of such measurements was limited due to lack of clarity and small size. Accordingly, the limitations in measurement accuracy may also account for the disparity in results.

CONCLUSION

The objectives of this project were to design and demonstrate the use of a goniometer to monitor hip position in cycling while standing. To assure that all data collected would be representative of realistic cycling situations certain design criteria had to be satisfied. Of the design criteria, the two that are most important are those concerning normal riding styles and accuracy. Allowing normal riding style as well as uninhibited transition from seated to standing posture is achieved by a design which measures hip position using spherical coordinates. Spherical coordinates enable a design with an extended radius which has a large enough range of motion to accommodate different riding postures. Since all three degrees of freedom are supported by low friction needle bearings, the goniometer does not inhibit normal riding styles. The fact that none of the riders noticed the goniometer during testing is evidence of this.

Errors that affect determining the position of the hip joint center are introduced by the goniometer, by soft tissue movements, by rotation of bones over which the goniometer is attached, and by anthropometric uncertainties. Of these, the inherent error introduced by the goniometer is the smallest (2.5 mm). Attaching the goniometer to the superior aspect of the greater trochanter along the femur axis of rotation during flexion/extension movements introduces potentially large soft tissue movement error ($\sim$2–3 cm) in the elevation coordinate. This error can be corrected in the data processing, however.

Further, enabled by a video-based motion analysis system, preliminary studies of leg movement during cycling while standing showed that potentially problematic femur rotations (axial and abduction/adduction) were minimal. As a consequence of correcting for soft tissue movement and of rotations being minimal, the absolute accuracy of all three position coordinates due to the various error sources is on the order of 1 cm.

The added degrees of freedom of the leg/bicycle linkage due to hip motion during cycling while standing has been a barrier to performing biomechanical analyses. By enabling measurement of hip motion, the goniometer presented in this paper overcomes this barrier. Accordingly, the stage is now set for performing the analyses necessary to advance understanding of cycling biomechanics while standing. Such analyses will be a subject of future work.

Acknowledgements—We wish to thank Shimano Corporation for its funding of this project and, in particular, Shinpei Okajima and Wayne Stetina.

REFERENCES

Ericson, M. O., Bratt, A., Nissell, R., Nemeth, G. and Ekholm, J. (1986) Load moments about the hip and knee joints during ergometer cycling. *Scand. J. rehabil. Med.* **18,** 165–172.

Hull, M. L. and Davis, R. R. (1981) Measurement of pedal loading in bicycling: I. Instrumentation. *J. Biomechanics* **14,** 843–856.

Komor, A., Dal Monte, A., Faina, M. and Leonardi, L. (1985) An attempt of modeling and computer simulation in optimization of an athlete. Report to the Institute of Sport Science, Rome, Italy. Part I.

Miller, T. A., Martin, P. E. and Wells, C. L. (1988) The effect of position and cadence on the biomechanical characteristics of hill climbing cyclists. *Proc. 12th Ann. Meet. Am. Soc. Biomechanics*, pp. 126–127, Champaign, Illinois.

Okajima, S. (1983) Designing chainwheels. *Bike Tech.* **2,** 1–7.

Redfield, R. and Hull, M. L. (1986) On the relation between joint moments and pedalling rates at constant power in bicycling. *J. Biomechanics* **21,** 317–329.

Sharp, A. (1896) *Bicycles and Tricycles.* Longmans Green (reprinted from M.I.T. Press, Cambridge, 1977).

Soden, P. D. and Adeyefa, B. L. (1979) Forces applied to a bicycle during normal cycling. *J. Biomechanics* **12,** 527–571.

Tylkowski, C. M., Simon, S. R. and Mansour, J. M. (1982) Internal rotation gait in spastic cerebral palsy. *Proc. 10th Open Sci. Meet. Hip Soc.* (Edited by Nelson, J. P.), Ch. 7, pp. 89–124. Mosby, St. Louis.

Wong, M. G. and Hull, M. L. (1983) Analysis of road induced loads in bicycle frames. *J. Mech. Transm. Autom. Design* **105,** 138–145.